

1 Potential Impacts of Future Climate Change and Emission on the
2 Fate and Transport of PFOS in the Bohai Rim, China

3 Chao Su ^{a, b}, Shuai Song ^a, Yonglong Lu ^{a*}, Baninla Yvette ^{a, b}, Shijie Liu ^a, John P. Giesy ^c,
4 Deliang Chen ^d, Alan Jenkins ^e, Andrew Sweetman ^{e, f}

5
6 ^a State Key Laboratory of Urban and Regional Ecology, Research Center for Eco-Environmental
7 Sciences, Chinese Academy of Sciences, Beijing 100085, China

8 ^b University of Chinese Academy of Sciences, Beijing 100049, China

9 ^c Toxicology Centre and Department of Veterinary Biomedical Sciences, University of
10 Saskatchewan, Saskatoon, Saskatchewan, Canada

11 ^d Department of Earth Sciences, University of Gothenburg, 405 30 Gothenburg, Sweden

12 ^e Centre for Ecology & Hydrology, Wallingford, OX 10 8BB, UK

13 ^f Lancaster Environment Centre, Lancaster University, Lancaster LA1 4YQ, UK

14
15 Corresponding author:

16 *Yonglong Lu

17 Tel: 86-10-62915537

18 Fax: 86-10-62918177

19 E-mail: yllu@rcees.ac.cn

20
21 **Abstract:**

22 Both climate change and contaminant emission rate are expected to affect the transport and fate of
23 POPs. However, studies on their integrative impacts are fewer. This study, taking Perfluorooctane
24 Sulfonate (PFOS) as an example, explored how future climate change and contaminant emission
25 affect the fate of POPs synthetically, as well as urbanization rate being taken into account, using
26 BETR-Urban-Rural (BETR-UR) model, an improved BETR model. The results suggested that
27 climate change had significant effects on the fate of PFOS, with precipitation and temperature

28 being predominant factors, by the following aspects: advection processes, degradation rate, and
29 intermedia transfer processes. Under the “business-as-usual” emission scenario, for most grids, a
30 remarkable decline in PFOS concentration was observed in fresh water and urban soil in the future,
31 particularly in the late 21st century, while coastal water and rural soil displayed an opposite
32 changing trend. Besides, under the integrative effects of reducing emission and climate change
33 scenarios, PFOS concentrations in each compartment decreased sharply over time. Additionally,
34 we discussed the influences of climate change on the fluxes of PFOS to the Bohai Sea. Total sum
35 of emissions increased by 1.61%, 11.80%, 17.04% with increasing precipitation, and sinks by
36 2.59%, 14.30%, 22.24% due to volatilization and degradation flux in 2035, 2065, and 2100,
37 respectively. However, the sum of the emissions was always more than the sum of the sinks in
38 Bohai Sea. The coastal or marine ecosystem should be given greater consideration in the future.
39 This suggests that future assessment of climate change impacts on POPs fate should take emission
40 reduction into consideration.

41 **Keywords:** climate change, emission rate, urbanization, PFOS fate, multimedia model, regional
42 scale

43 1. Introduction

44 Persistent organic pollutants (POPs) are a kind of pollutants with the following properties:
45 persistence, toxicity, and long-range atmospheric transport (LRAT). Due to these properties,
46 particularly the LRAT resulting in dispersed contamination far from source regions, the fate and
47 behavior of POPs have captivated increasing concern from international environmental
48 organizations, governments, academics, and the public. Many researches showed that the fate and
49 behavior of POPs have been affected by various factors, e.g. emission rate, environmental
50 parameters such as temperature, rain rate, and soil solids organic carbon fraction. (Prevedouros et
51 al., 2004a; Prevedouros et al., 2004b). Climate change is having far-reaching effects on the
52 environment and then on the fate of POPs, not only impacted by and impacting on natural
53 processes within the climate system itself, but also anthropogenic activities (e.g., increased
54 emissions of greenhouse gases) (Paul et al., 2012). Direct changes such as temperature rise, and
55 those driven by it (ocean temperature rise, sea-level rise), altered precipitation patterns, wind and

56 ocean current patterns, hence resulted in those indirect changes such as land cover changes.

57 In general, the influencing mechanism of climate change on the environmental behavior and
58 fate of POPs could be described from three aspects. Firstly, it is likely to influence the
59 environmental behavior of POPs by enhancing the volatilization from primary and secondary
60 sources, by influencing their partitioning between soil, sediment, water, and atmosphere, including
61 air-surface exchange, wet/dry deposition, and reaction rates (Teran et al., 2012). Secondly, it could
62 change the solubility of chemicals, and consequently change their concentration and activity in the
63 environment. Then, it could affect the decomposition rate of POPs in the environment (Zhou and
64 Ma, 2013). However, our understanding of these mechanism is mostly qualitative, and a more
65 quantitative description of potential effects is needed (Woehrschimmel et al., 2013). Recently, a
66 few studies have explored the effects using models under climate change scenarios quantitatively
67 (Gouin et al., 2013; Lamon et al., 2009; Ma and Cao, 2010; Paul et al., 2012). Lamon et al. studied
68 fate and transport of PCBs under a realistic climate change scenario using global multimedia
69 model under steady state (Lamon et al., 2009). On regional scale, Paul et al. and Henry et al.
70 explored the potential implications of future climate and land-cover changes for the fate and
71 distribution of POPs in Europe and Arctic, respectively (Paul et al., 2012; Woehrschimmel et al.,
72 2013). The common modeled results showed that the effect of climate change on environmental
73 concentrations of POPs was typically up to factors between 1.5 and 2.5 even up to 4 in modeled
74 concentrations. While, PCB 153 displayed a change with the most reduction in burden of up to 40%
75 in some Mediterranean compartments in Europe (Paul et al., 2012). However, the researches
76 combining climate change and emission rate to study the integrated effects are fewer.

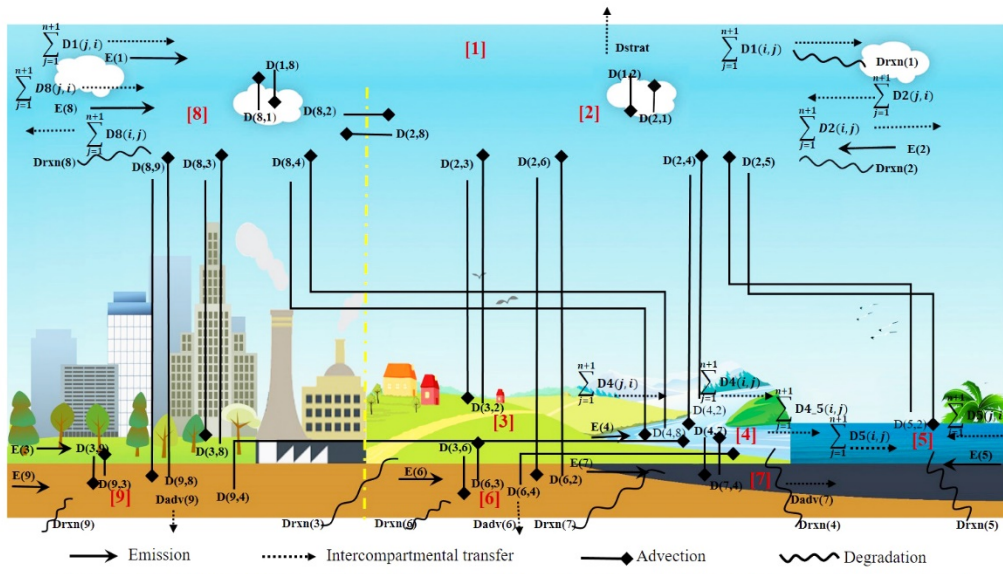
77 The objective of this study is to explore how climate change (temperature, precipitation, wind
78 speed, soil carbon stock, and sea-level rise) and emission rate affect the fate of perfluorooctane
79 sulfonate (PFOS), as well as the urban-rural disparities, with a focus on Bohai Rim in China. In
80 this study, the Berkeley-Trent-Urban-Rural (BETR-UR) model was used to run the simulations
81 under the three climate change scenarios (B1, A1B, and A2) in IPCC 2007 and four emission
82 scenarios for three 20-year periods throughout the 21st century (2016-2035, 2046-2065, and
83 2081-2100), relative to the baseline simulation of 2010. Then, it explored the key affecting factors
84 of PFOS, and analyzed the alterations of mass fluxes of PFOS to the Bohai Sea under climate
85 change. This research could provide powerful theoretical support for PFOS emission reduction

86 and ecosystem protection.

87 2. Methods and Materials

88 2.1 Model description and study area

89 Within the original BETR model based on fugacity concept (Mackay, 2001), a connected
90 system of nine discrete and homogeneous compartments is considered as one segmentation (or
91 grid). BETR model has been successfully applied to model the multimedia fate of chemicals,
92 including the North America (MacLeod et al., 2001; Woodfine et al., 2001), Europe (Prevedouros
93 et al., 2004a; Prevedouros et al., 2004b), and the global environment (MacLeod et al., 2005). The
94 BETR-UR model is an improved BETR model (Song et al., 2016). It takes the effects of
95 urbanization into account, dividing the soil and lower air compartments into urban soil and rural
96 soil, lower urban air and lower rural air, respectively. The urban areas mainly indicated those areas
97 with high population density, including industrial land, built-up land, commercial districts, urban
98 residential areas, municipal land for public facilities, and their buffers. Except for urban areas, we
99 defined rural areas as a combination of rural villages, agricultural land, grassland, forest land, rural
100 residential areas, unused land and so on (Wang et al., 2010). The framework of BETR-UR model
101 is illustrated in Fig. 1. In the BETR-UR model, the environment within each segment contains
102 nine compartments. Specific environmental parameters for an urban area like urban perimeter,
103 urban-rural atmospheric mixing rate, freshwater area of urban area etc. and transfer processes
104 between urban and rural area were also improved. More materials could be found in (Song et al.,
105 2016).



[1] Upper Air, [2] Rural Air, [3] Vegetation, [4] Fresh Water, [5] Coastal Water, [6] Rural Soil, [7] Fresh Water Sediment, [8] Urban Air, [9] Urban Soil

106

107

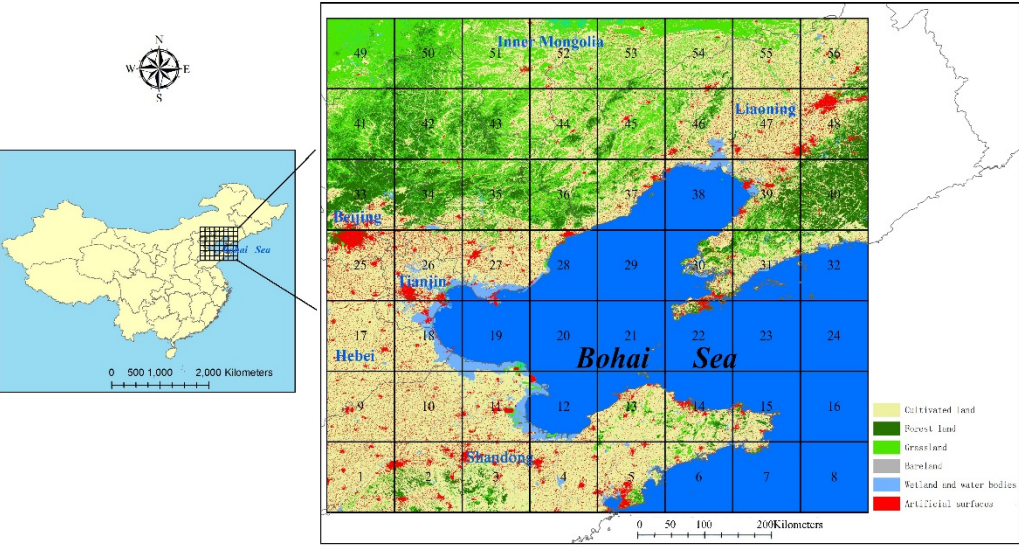
Fig. 1 Contaminant transportation processes in the region i linked with j in the BETR-UR model.

108

109

The Bohai Rim, including part of Bohai Sea and its surrounding area, is one of the most prosperous regions in China. In this paper, the study area included Beijing, Tianjin, Liaoning, Hebei and Shandong provinces and municipalities. A wide range of industries are distributed in this region, including textile treatment, metal plating, production of firefighting chemicals and semiconductor industries, some of which are associated with industrial sources of PFOS and related substances in China (Xie et al., 2013b). Rapid urbanization and industrial development have caused great increase in energy consumption and pollutants emission, further leading to multiple environmental problems.

116



117

118

Fig. 2 Study area and model segmentation.

119 The longitude of Bohai Rim is from 116°E to 124°E, and the latitude is from 36°N to 43°N.
 120 It is divided into 56 grids by 1°×1° (Fig. 2). For the study area, each grid contained 8
 121 compartments which are lower rural air, lower urban air, rural soil, urban soil, fresh water, fresh
 122 water sediment, coastal water, and vegetation. The effects of upper air were ignored as the
 123 influence of long-range air transport within this region was considered to be limited. The 56
 124 sub-grids are linked by advection of air, fresh water and coastal water between adjacent segments,
 125 and the runoff of fresh water to coastal water was also considered.

126 2.2 Physico-chemical properties of PFOS

127 PFOS, as one of the most abundant old-generation members of PFAS family, is a kind of
 128 emerging POPs, and is one of the pollutants that are most difficult to degrade. PFOS and related
 129 substances are synthesized chemicals manufactured for their desirable properties of chemical
 130 stability, high surface activity, and water and oil repellence (Giesy and Kannan, 2001, 2002).
 131 China began to produce PFOS-based products at a large scale in 2004, and the annual production
 132 of PFOS-related chemicals grew rapidly from 2003 to 2011 (Xie et al., 2013a). The
 133 physical-chemical properties of PFOS included in the BETR model are listed in Table 1 (Liu,
 134 2014). Additionally, in view of both hydrophobic and hydrophilic properties of PFOS (Brooke et
 135 al., 2004), improvements were made to the calculation of PFOS partition coefficient due to the
 136 influence of water salinity on the sorption behavior. Full details are available in the study by (Liu
 137 et al., 2015).

138

Table 1 Physico- chemical properties of PFOS

Properties	MW	M.P.	Solub	V.P.	Log(K_{OW})	Log(K_{OA})	$\tau_{1/2}$ LA
PFOS	538.54	400.00	519.00	3.31E-04	4.88	11.73	265500
Properties	$\tau_{1/2}$ Soil	$\tau_{1/2}$ Veg.	$\tau_{1/2}$ FW.	$\tau_{1/2}$ CW.	$\tau_{1/2}$ Sed.	E.P.	E.S.
PFOS	100000000	265500	5500000	5500000	17000000	50000	-20000

139 Notes: molar mass (MW, g/mol), melting point (M.P., °C), aqueous solubility (Solub, g/m³), vapor
 140 pressure (V.P., Pa), lower air reaction half-life ($\tau_{1/2}$ LA, h), soil reaction half-life ($\tau_{1/2}$ Soil, h),
 141 vegetation reaction half-life ($\tau_{1/2}$ Veg., h), fresh water reaction half-life ($\tau_{1/2}$ FW., h), coastal water

142 reaction half-life ($\tau_{1/2}$ CW., h), sediment reaction half-life ($\tau_{1/2}$ Sed., h), enthalpy of vaporization
143 from water to air (E.P., J/mol) and enthalpy of solution from octanol to water (E.S., J/mol).

144 2.3 Emission scenarios

145 According to the methodology and emission inventory developed by our research group (Xie
146 et al., 2013a; Xie et al., 2013b), spatially distributed emissions of PFOS and its related
147 substances were estimated for the study area in 2010, which was under the hypothesis that all
148 PFOS related substances immediately degraded to PFOS (Liu et al., 2015). In this study, four
149 different future emission scenarios were proposed for the three 20-year periods to the year 2100.
150 The emission scenario 1 is called “business-as-usual (BAU)” scenario, under the assumption that
151 annual PFOS emission continues in the future till 2100. Since PFOS and its related substances
152 were listed in Stockholm Convention on POPs in 2009, the production of PFOS-related chemicals
153 fluctuated and stabilized at around 250 t/a in China from 2009 (Xie et al., 2013b). So the PFOS
154 emission till 2100 was assumed to be the same as in 2010. This is also a reference scenario in
155 order to explore the effects of climate change. Under this assumption, the emissions to each
156 compartment including fresh water, urban soil, rural soil, urban air, and rural air kept constant.
157 The reason for this assumption is that, it is easier to manage and implement the pollution control
158 measures in urban areas even if the population and land-use area of urban areas would increase till
159 2100. For rural areas, even though the population and land-use area would decrease by time (more
160 details are referred to Section 2.4), along with the shift of industrial development from urban to
161 rural areas and the improvement of people’s living standard, the industrial and domestic emissions
162 would almost continue.

163 The emission scenarios 2, 3, and 4 are on the hypothesis that China would begin to phase
164 out PFOS and similar chemicals, and use alternatives fully by 2030, 2050, and 2100, respectively,
165 in compliance with the international treaties and national regulations. It is assumed that the PFOS
166 emission would linearly decrease to zero from 2016 until the year of withdrawal. Since the
167 Chinese government set a series of regulations on the production and use of PFOS in 2014 to
168 abide to the Stockholm Convention, thus encouraging the development of alternatives, while it did
169 not determine the withdrawal year, we set the above three scenarios in this study. After the

170 withdrawal year, releases will not be suddenly stopped because of applications by secondary users.
171 For all secondary users (metal plating, firefighting, textile, semiconductor, and domestic users), a
172 worst-case situation is given in which the storage of each one was within its shelf life and all
173 expired products would be treated on time. Hence, emissions from storage of secondary products
174 would continue being released during shelf-life period. Remarkably, there are some differences
175 between industrial sectors and domestic users in the future emission. For industrial sectors, taking
176 fire-fighting sector as an example, the shelf life of products is 5 years, then the releases would be
177 as the same as the previous for 5 years. For domestic applications, releases would be assumed to
178 reduce linearly as products come to the end of their natural life. For example, carpets are in use for
179 an average of about 10 years, releasing one tenth of their treatment each year until eventual
180 disposal (Paul et al., 2008). In addition, PFOS-polymers released from textile processes would
181 degrade after 30 years, because the half-life of PFOS-polymers is longer and even more than 30
182 years, and the transforming factor was 0.3 (Brooke et al., 2004). Finally, the future simulations of
183 the three 20-year periods were under the annual mean emission of each period. The estimated total
184 emissions of PFOS and their compartment distributions for the four scenarios are listed in Table
185 S1.

186 2.4 Brief introduction to climate change and urbanization scenarios

187 The following changes were implemented for each climate change scenario (Special Report
188 on Emission Scenarios (SRES) B1, A1B, and A2 in IPCC 2007): precipitation, temperature,
189 sea-level rise, soil carbon stock, and wind speed. The SRES scenarios explore alternative
190 development pathways, covering a wide range of demographic, economic and technological
191 driving forces and resulting greenhouse gas emissions. B1 describes a convergent world, a global
192 population that peaks in mid-century, but with more rapid changes in economic structures toward
193 a service and information economy. The A1B assumes a world of very rapid economic growth, a
194 global population that peaks in mid-century and rapid introduction of new and more efficient
195 technologies but a balance across all sources. A2 describes a very heterogeneous world with high
196 population growth, slow economic development and slow technological changes. The global
197 average best estimate temperature changes at 2090-2099 relative to 1980-1999 were 1.8°C, 2.8°C,

198 3.4□ for those three scenarios, respectively. More introductions about SRES B1, A1B, and A2
199 could be found in IPCC Climate Change 2007 Synthesis Report (IPCC, 2007). In this paper, the
200 climate change scenarios were referred to some literatures focused on China of which the results
201 were based on IPCC 2007. More details are as follows.

202 ● Precipitation

203 Gridded 10-year averaged precipitation rates in the study area were extracted from (Zhang et
204 al., 2012) for the periods 2016-2035, 2046-2065, and 2081-2100 (short of 2035, 2065, 2100 the
205 following, also called early, mid, and late 21st century respectively). Precipitation was projected to
206 increase over the study area by 3%-9% (10 yr)⁻¹, 7.5%-18% (10 yr)⁻¹, and 9%-18% (10 yr)⁻¹
207 respectively, under all three scenarios for the three periods.

208 ● Temperature

209 The same process was repeated for surface air temperature (Zhang et al., 2012). The warming
210 rate was projected to increase over the study area by 0.2-0.6□ (10 yr)⁻¹, 0.3-0.6□ (10 yr)⁻¹, and
211 0.1-0.6□ (10 yr)⁻¹ respectively, under all three scenarios for the three periods. Additionally, the
212 significant feature of urbanization is “urban heat island effect”, and the temperature difference
213 between urban and rural area was 2-6□ (Martine and Marshall, 2007). Hence, this effect was
214 taken into account in the BETR-UR model, and it was assumed to be 4□ for that difference.

215 ● Sea-level rise

216 The mean rate of averaged sea-level rise in China was 3.0 mm yr⁻¹ between 1980 and 2014. It
217 was inferred that the sea-level of Bohai Sea in the early 21st century was 0.045 m higher than that
218 in 2010 for all three scenarios (China Sea Level communique 2014). The sea-level rise in mid and
219 late 21st century was referred to the global mean data in IPCC AR5, being 0.26 m, 0.25 m, 0.30 m
220 and 0.47 m, 0.48 m, 0.63 m higher under three scenarios, respectively (IPCC, 2014).

221 ● Soil carbon stock

222 The simulated averaged soil carbon stock increased by 5% for 2030s, and by 3% for 2090s
223 under scenarios B1 and A2 for northeastern China (Peng et al., 2009). Hence, it is assumed that it
224 increased by 4% for the 2060's under those two scenarios. Furthermore, since scenario A1B is a
225 moderate one between B1 and A2, we supposed that projected averaged soil C stock had the same
226 growth with those two scenarios. Additionally, a study showed that soil carbon stock was about
227 57.76% lower in urban land than that in non-construction land (forest land and green open spaces)

228 (Tao et al., 2015), which was taken into consideration in the model.

229 ● Wind speed change

230 A study using all climate model predicted that the annual mean wind speeds in China for the
231 21st century varied slightly under all three scenarios (Jiang et al., 2010). It was projected that mean
232 wind speed increased 0-1 m/s under the three scenarios for the early, mid and late 21st century in
233 the northern part of Northeastern China, middle reaches of the Yellow River and southwest of
234 Tibetan Autonomous Region. Moreover, it increased a little more under scenario A2 than the other
235 two scenarios, and it also increased more in the mid and late 21st century than the early 21st
236 century (Jiang et al., 2010). In this paper, we considered that it had a similar change pattern in the
237 Bohai Rim and northern part of Northeastern China, middle reaches of the Yellow River.

238 Besides, rainfall-runoff relationship and urbanization rate projections were analyzed. The
239 former was referred to the regression model relating mean annual runoff to mean annual
240 precipitation and mean annual temperature by (Chen and Wang, 2004). Rapid urbanization is one
241 of the outstanding features in China, particularly in coastal regions, and China is now at the peak
242 of its urban transition, where rural-urban migration has been a much more important contributor to
243 the growth (Martine and Marshall, 2007). Urban form and function also help define the nature of
244 the interactions between cities and local climate change. For example, the “urban heat island effect”
245 resulting from the impacts of different land uses in urban areas, creates microclimates and health
246 consequences. The size of the urban center, the type of urbanization, urban form, function and
247 land use all contribute to the effect. As villages grow into towns and then into cities, their average
248 temperature increases from 2 to 6 °C above that of the surrounding rural areas (Martine and
249 Marshall, 2007). Since the percentile urbanization trend of Asia from 2000 to 2050 was almost
250 consistent with the curve of urban percentage of Europe from 1950 to 2000, we therefore, assumed
251 that the rate of urbanization of China from 2051 to 2100 was likely the same as that of Europe
252 from 2000 to 2050 (Das Gupta et al., 2014).

253 3. Results and discussion

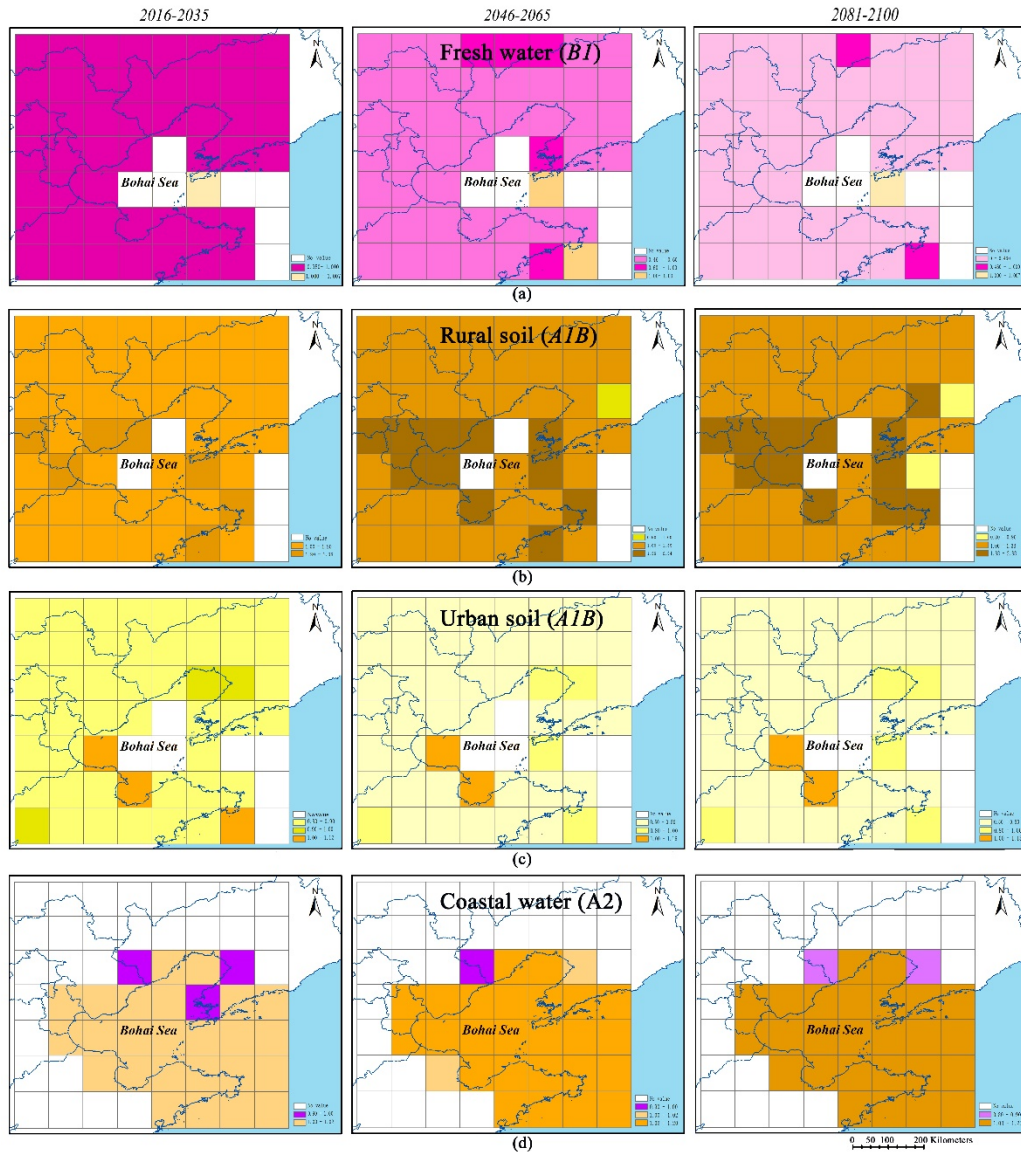
254 3.1 Model output and validation

255 The simulations were run 18 times on steady state solutions, under each climate change

256 scenario for each emission scenario. The previous research showed that soil, coastal water, fresh
257 water, and sediment were the top four sinks for PFOS, and the storage in air and vegetation was
258 less than 1.00 %. Consequently, the concentrations and transfer process in urban soil, rural soil,
259 coastal water, fresh water, and sediment were mainly analyzed in the results of this study. The
260 median values of modeled PFOS concentrations in 2010 in fresh water, sediment, urban soil, and
261 rural soil were 8.27 ng/L, 0.38 ng/g, 0.26 ng/g, and 0.11 ng/g, respectively. Additionally, model
262 accuracy was assessed by comparing simulated baseline PFOS concentrations with measured data
263 in fresh water, fresh water sediment, urban soil, and rural soil in the study area (Table S1).
264 Available measured data for PFOS concentrations around the year 2010 were collected from
265 published sources, mostly by our research group (Li et al., 2011; Meng et al., 2015; Wang et al.,
266 2014; Wang et al., 2015; Yang et al., 2011; Zhao et al., 2014; Zhao et al., 2013; Zhu et al., 2014).
267 The results showed that the range of simulated concentrations were generally well consistent with
268 the measured data for all the compartments.

269 3.2 Spatially projected concentration changes of PFOS

270 3.2.1 Projected concentration changes of PFOS under emission scenario 1



271

272

Fig. 3 Projected changes of PFOS concentrations in fresh water, rural soil, urban soil and

273

coastal water under specific climate change scenario for emission scenario 1.

274

275

Ratio of projected period concentration and baseline concentration was used to describe the change of PFOS concentration in this study.

277

278

Concentration changes of PFOS for fresh water, coastal water, urban soil, and rural soil under three future climate change scenarios and four emission scenarios were listed in Table S3. It showed that there were similar changing trend for those four compartments among three climate

280

change scenarios B1, A1B and A2 under each specific emission scenario. Fig. 3 showed the

281

projected changes of PFOS concentrations in those four compartments under specific climate

282

change scenario for emission scenario 1. It could be seen that a remarkable decrease in PFOS

283 concentration in the future simulations was observed in fresh water and urban soil (except for
284 some grids). Taking grid 26 (Haihe River in Tianjin City) as an example, the concentration ratios
285 in the early, mid, and late 21st century for fresh water were 0.9616, 0.5394, 0.2772, and for urban
286 soil were 0.8708, 0.7530, 0.7533 under climate change scenario B1. And under scenarios A1B and
287 A2, fresh water concentration ratios were 0.9414, 0.4849, 0.2529 and 0.9750, 0.5203, 0.3179 in
288 the future three periods, the urban soil concentration ratios were 0.8698, 0.7515, 0.7546 and
289 0.8693, 0.7504, 0.7537 in the future three periods, respectively. Fresh water was observed with the
290 most rapid decline. The key reason for that was the increased runoff with increasing precipitation
291 even though it brought the PFOS in air to aquatic and terrestrial ecosystems through wet
292 deposition and rain dissolution with the increasing precipitation. According to the regression
293 relationship between runoff and precipitation, temperature (Chen and Wang, 2004), the runoff
294 increased a lot, particularly for the mid, and late 21st century, with a value by 5%, 25%, 32% in the
295 future three periods, respectively, under scenario B1. On the other hand, warming water would
296 reduce the solubility of PFOS (Zhou and Ma, 2013). For the urban soil, it might be because the
297 industrial and domestic emissions kept constant under the assumption of industrial shift from
298 urban to rural areas and managed domestic consumptions while with the higher urbanization rate
299 and extended urban land. On the other hand, concentrations of PFOS would decline driven by
300 temperature increasing volatilization and microbial decomposition rate. And this volatilization
301 effect driven by temperature was more significant in urban areas than rural areas because of the
302 urban heat island effect.

303 On the contrary, for most grids, the concentrations of PFOS in rural soil and coastal water
304 had the opposite trends. Taking grid 26 (Tianjin City) as an example, for rural soil, the
305 concentration ratios were 1.1705, 1.3855, 1.4618 in the future three periods under scenario A1B,
306 and the ratios for coastal water were 1.0029, 1.1688, 1.2259 under scenario A2 in the future three
307 periods, respectively. For coastal water, the runoffs from fresh water to coastal water increased
308 greatly owing to the higher temperature and precipitation, with a value of 14%, 32%, and 38% in
309 the future three periods, respectively. This would bring out the accumulation of PFOS in coastal
310 water. It was consistent with that coastal water was the final sink for PFOS (Liu et al., 2015). For
311 rural soil, under the BAU emission assumption that the related domestic consumptions increased
312 and industries clustered in rural areas while the population and land-use areas decreased in section

313 2.3, it was reasonable to show a higher concentration in the future.

314 3.2.2 Projected concentration changes of PFOS under emission reduction scenarios

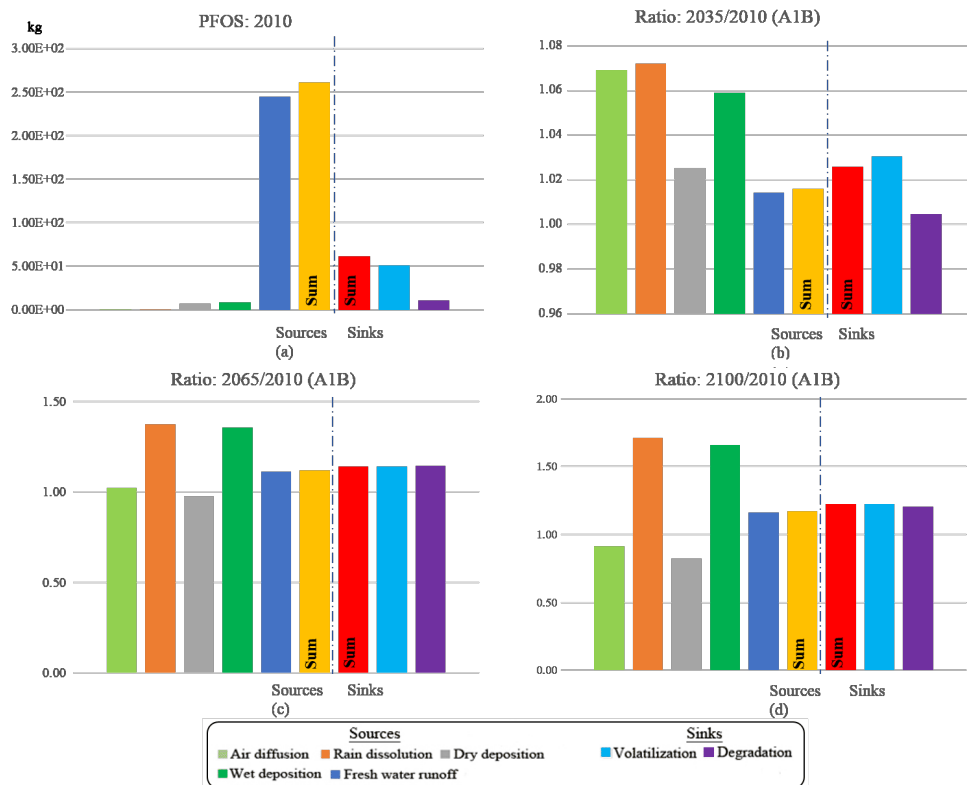
315 Fig. S1- S3 showed the projected changes of PFOS concentrations in fresh water, rural soil,
316 urban soil and coastal water under specific climate change scenario for emission scenarios 2, 3 and
317 4. For emission scenario 2, the PFOS concentrations in fresh water in the whole area will decrease
318 65% or above in the early 21st century. However, in the mid 21st century, there will be some
319 growth in the southern Bohai Rim comparing to the early 21st century, and for a small number of
320 grids, the PFOS concentrations are higher than 2010. This was closely related to the emission of
321 PFOS. Because in the mid 21st century, the PFOS emission will only be from textile sector, and
322 which in the grids of southern Bohai Rim is higher than the early 21st century under the
323 assumption of emission scenario 2. For rural soil and urban soil, the PFOS concentrations will
324 decrease in the early 21st century, and decrease more in the mid 21st century except for a tiny
325 number of grids. And coastal water is the final sink of PFOS, for a big number of grids, the
326 concentrations are higher than the early 21st century, even for 2010. The trends of other three
327 compartments are almost consistent with the fresh water, because fresh water is the only medium
328 of PFOS released into the environment in the mid 21st century (Fig. S1 and Table S3).

329 For emission scenarios 3 and 4, the PFOS concentrations in the four compartments will
330 reduce with the linear emission reduction over time except for a few grids. Particularly for
331 emission scenario 3, with the PFOS withdrawn in 2050, the PFOS concentrations will decrease a
332 lot in the late 21st century, by 10 to 10,000-fold (Fig. S2, S3 and Table S3).

333 3.3 Annual mass flux changes of PFOS in Bohai Sea

334 In order to explore the impacts of climate change on the fluxes of PFOS to the Bohai Sea,
335 total annual mass flux changes were discussed under emission scenario 1 and climate change
336 scenario A1B because it was a moderate choice.

337



338

339 Fig. 4 Total annual mass fluxes (kg), to the Bohai Sea, sources and sinks for (a) 2010. Ratios of
 340 total annual mass fluxes: (b) 2035/2010, (c) 2065/2010, and (d) 2100/2010 under scenario A1B.

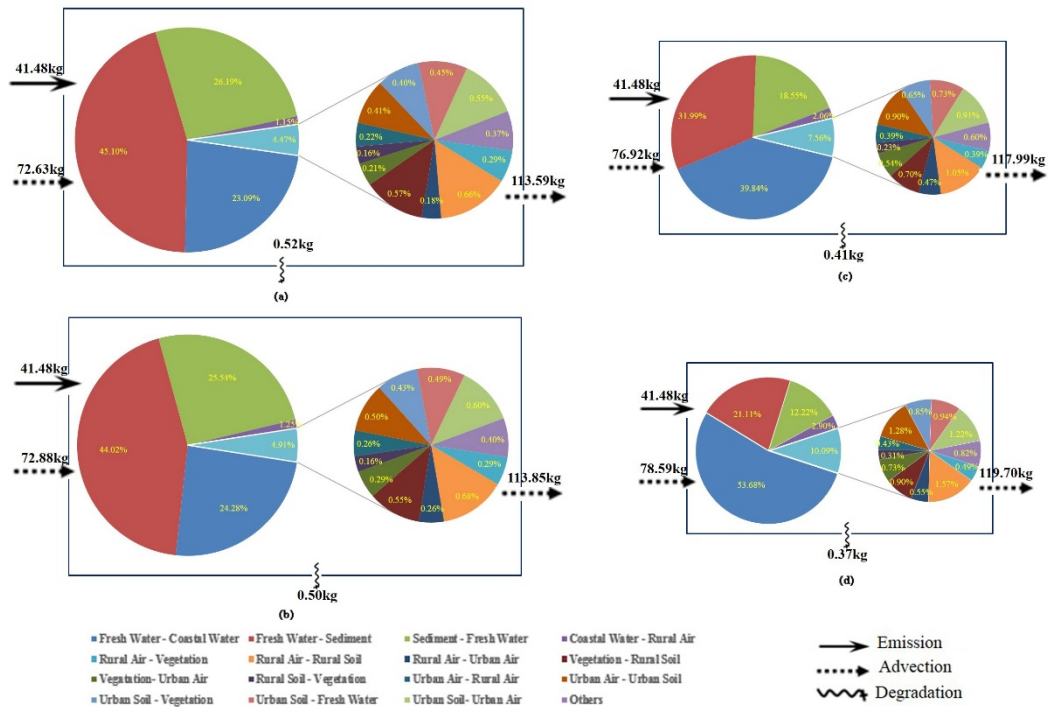
341

342 Total annual mass fluxes of PFOS to the Bohai Sea for baseline 2010, and the ratios of the
 343 fluxes for the years 2035/2010, 2065/2010 and 2100/2010 were presented in Fig. 4.

344 For pathways of PFOS to the Bohai Sea, rain dissolution, wet deposition, and fresh water
 345 runoff all will increase somehow in the three future periods, relative to the baseline 2010. Rain
 346 dissolution will be up by 7.21%, 37.39%, 71.00%, wet deposition will increase in ascending order
 347 by 5.91%, 35.62%, 65.94%, while fresh water runoff will increase by 1.42%, 11.39, 16.30% in
 348 2035, 2065, and 2100, respectively, relative to 2010. These changes are due to increased
 349 precipitation in the future. Air diffusion and dry gas deposition firstly increase a little in 2035,
 350 then decrease more in 2065 and 2100, remains lower than volatilization and degradation. For sink
 351 pathways, volatilization and degradation fluxes both will increase more in the future, relative to
 352 the present (2010). This is because of the increased air and water temperature and wind speed.
 353 Total sum of sources will increase by 1.61%, 11.80%, 17.04%, and that of sinks by 2.59%,
 354 14.30%, 22.24% in 2035, 2065, and 2100, respectively. However, the sum of sinks in 2010 was

355 much lower than the sum of sources to the Bohai Sea, so the sum of the sources (left side of the
 356 dotted line) is always more than the sum of the sinks (right side of the dotted line), and the
 357 differences between the sum of the sources and the sum of the sinks will be larger in the future.
 358 This added to the evidence that PFOS concentrations in coastal water would increase more in the
 359 future periods. It was inconsistent with the modeled results of γ -HCH and PCB 153 in the North
 360 Sea (O'Driscoll et al., 2014). So the general result was that there were big influences of climate
 361 change on the mass fluxes of PFOS to the Bohai Sea.

362 3.4 The changes of PFOS fate and transportation: taking Tianjin city as a case



363
 364 Fig. 5 The changes of PFOS fate and transportation of grid 26 under emission scenario 1 and
 365 moderate climate change scenario A1B : (a) baseline 2010; (b) 2016-2035; (c) 2046-2065; (d)
 366 2081-2100.

367 In this part, we took grid 26 (containing the vast majority of Tianjin City) as an example to
 368 analyze the impacts of future climate change (scenario A1B) on the fate and transportation of
 369 PFOS in detail, including advection fluxes between adjacent grid (inflow/outflow fluxes of air),
 370 degradation rate, and intermedia transportation processes (Fig. 5). Under emission scenario 1, due
 371 to the increasing mean wind speed, both the inflow and outflow fluxes will increase, particularly

372 in the mid and late 21st century, by 5.91%, 8.21% for inflow flux, and 3.87%, 5.38% for outflow
373 flux. For the not temperature dependent degradation rate, it will decline slightly with time.
374 Because the degradation rate is a complex parameter, relating to the volume of each environmental
375 compartment, PFOS concentration in each compartment, and the first-order reaction rate constant
376 (Mackay, 2001; MacLeod et al., 2001). The value in Fig. 5 was the sum of all environmental
377 compartments, hence, its reduction was maybe closely linked with the decrease of PFOS
378 concentration in fresh water, fresh water sediment, urban soil, volume of rural soil, and rural air.

379 For the intermedia transportation processes, we could see that from fresh water to coastal
380 water, fresh water to sediment, sediment to fresh water, and coastal water to rural air were the four
381 predominant transfer ways among all transfer processes (Fig. 5). Among these four pathways, the
382 transfer rate of fresh water to coastal water, coastal water to rural air increases over time,
383 particularly for the former, from 1/4 of the total in 2010 to more than half in the late 21st century.
384 It is because of increased runoffs from fresh water to coastal water led by more and more
385 precipitation in the mid and later 21st century. For the transfer rate of coastal water to rural air, it is
386 driven by temperature increasing volatilization. The transfer rate of the other two predominant
387 pathways will reduce much in the future, especially in the mid and late 21st century, decreasing by
388 5.62% - 74.55% for fresh water to sediment, and 5.73% - 74.62% for sediment to fresh water, in
389 the future (Fig. 5). According to the transfer principle between fresh water and sediment, along
390 with the concentration reduction in fresh water, the concentration in sediment will also decrease,
391 as well as the transfer rate between them.

392 4. Conclusion

393 This paper explored the potential integrative effects of future climate change and emission
394 rate on the fate and transportation of PFOS in the Bohai Rim of China using BETR-UR model,
395 taking the effects of urbanization into consideration at the same time. Our results suggested that
396 wind speed, degradation rate, and intermedia transfer processes affect PFOS advection processes.
397 Under the influences of climate change (including temperature, precipitation, wind speed,
398 sea-level rise, and soil carbon stock) and urbanization, the projected concentrations of fresh water
399 and urban soil would decrease a lot in the future, potentially lowering the exposure burden of biota

400 in fresh water and urban soil. These reductions were predicted to result from increased
401 temperature, precipitation, and urbanization. While that of coastal water and rural soil displayed
402 an opposite trend, which would bring out more adverse effects and risk on organisms, particularly
403 for marine ecosystem. Besides, there were big influences of climate change on the mass fluxes of
404 PFOS to the Bohai Sea. It is important to point out that these predicted changes would occur under
405 BAU emission. However, through modern, effective chemical management practices and
406 legislation, chemicals with PFOS-like properties might be effectively regulated and reduced, and
407 then concentrations of PFOS in each compartment would sharply decline and lower the risk on
408 ecosystems. It suggests that in the future emission reduction policy-making process, climate
409 change mitigation and adaptation should be taken into serious consideration, as well as
410 urbanization planning.

411

412 Acknowledgement

413 This study was supported by the International Scientific Cooperation Program with Grant No.
414 2012DFA91150, the National Natural Science Foundation of China under Grant No.
415 414201040045 and No. 41371488, and the Key Project of the Chinese Academy of Sciences under
416 Grant No. KZZD-EW-TZ-12. We would like to thank the editors and reviewers for their valuable
417 comments and suggestions.

418 References

419 China Sea Level communique 2014. China Sea Level communique. China Oceanic
420 Administration.

421 Brooke, D., Footitt, A., Nwaogu, T., 2004. Environmental risk evaluation report:
422 Perfluorooctanesulphonate (PFOS). Environment Agency Wallingford.

423 Chen, L., Wang, H., 2004. Sensitivity of Runoff to Climate Change in Small Drainage Basins in
424 China. Resources Science 26, 62-68.

425 Das Gupta, M., Engelman, R., Levy, J., Gretchen, L., Merrick, T., Rosen, J.E., 2014. The Power

426 of the 1.8 billion, ADOLESCENTS, YOUTH AND THE TRANSFORMATION OF THE
427 FUTURE, State of world population, 2014. UNFPA, <https://www.unfpa.org/sites/default/files/pub-pdf/SWOP>.

428

429 Giesy, J.P., Kannan, K., 2001. Global distribution of perfluorooctane sulfonate in wildlife.
430 Environmental science & technology 35, 1339-1342.

431 Giesy, J.P., Kannan, K., 2002. Peer reviewed: perfluorochemical surfactants in the environment.
432 Environmental science & technology 36, 146A-152A.

433 Gouin, T., Armitage, J.M., Cousins, I.T., Muir, D.C., Ng, C.A., Reid, L., Tao, S., 2013. Influence
434 of global climate change on chemical fate and bioaccumulation: The role of multimedia models.
435 Environmental Toxicology and Chemistry 32, 20-31.

436 IPCC, 2007. Synthesis Report. Contribution of Working Groups I, II and III to the Fourth
437 Assessment Report of the Intergovernmental Panel on Climate Change. IPCC, Geneva,
438 Switzerland.

439 IPCC, 2014. CLIMATE CHANGE 2014 SYNTHESIS REPORT.

440 Jiang, Y., Luo, Y., Zhao, Z., 2010. Projection of Wind Speed Changes in China in the 21st
441 Century by Climate Models. Chinese Journal of Atmospheric Sciences 34, 323-336.

442 Lamon, L., von Waldow, H., MacLeod, M., Scheringer, M., Marcomini, A., Hungerbühler, K.,
443 2009. Modeling the global levels and distribution of polychlorinated biphenyls in air under a
444 climate change scenario. Environmental science & technology 43, 5818-5824.

445 Li, F., Sun, H., Hao, Z., He, N., Zhao, L., Zhang, T., Sun, T., 2011. Perfluorinated compounds in
446 Haihe River and Dagu drainage canal in Tianjin, China. Chemosphere 84, 265-271.

447 Liu, S., 2014. Simulation of Spatial Explicit Multimedia Fate of POPs in Bohai Rim. University of
448 Chinese Academy of Sciences.

449 Liu, S., Lu, Y., Xie, S., Wang, T., Jones, K.C., Sweetman, A.J., 2015. Exploring the fate, transport
450 and risk of Perfluorooctane Sulfonate (PFOS) in a coastal region of China using a multimedia
451 model. Environment international 85, 15-26.

452 Ma, J., Cao, Z., 2010. Quantifying the perturbations of persistent organic pollutants induced by
453 climate change. Environmental science & technology 44, 8567-8573.

454 Mackay, D., 2001. Multimedia environmental models: the fugacity approach. CRC press.

455 MacLeod, M., Riley, W.J., Mckone, T.E., 2005. Assessing the influence of climate variability on

456 atmospheric concentrations of polychlorinated biphenyls using a global-scale mass balance model
457 (BETR-Global). *Environmental science & technology* 39, 6749-6756.

458 MacLeod, M., Woodfine, D.G., Mackay, D., McKone, T., Bennett, D., Maddalena, R., 2001.
459 BETR North America: a regionally segmented multimedia contaminant fate model for North
460 America. *Environmental Science and Pollution Research* 8, 156-163.

461 Martine, G., Marshall, A., 2007. State of world population 2007: unleashing the potential of urban
462 growth, *State of world population 2007: unleashing the potential of urban growth*. UNFPA.

463 Meng, J., Wang, T., Wang, P., Zhang, Y., Li, Q., Lu, Y., Giesy, J.P., 2015. Are levels of
464 perfluoroalkyl substances in soil related to urbanization in rapidly developing coastal areas in
465 North China? *Environmental Pollution* 199, 102-109.

466 O'Driscoll, K., Mayer, B., Su, J., Mathis, M., 2014. The effects of global climate change on the
467 cycling and processes of persistent organic pollutants (POPs) in the North Sea. *Ocean Sci* 10, 397.

468 Paul, A.G., Hammen, V.C., Hickler, T., Karlson, U.G., Jones, K.C., Sweetman, A.J., 2012.
469 Potential implications of future climate and land cover changes for the fate and distribution of
470 persistent organic pollutants in Europe. *Global Ecology and Biogeography* 21, 64-74.

471 Paul, A.G., Jones, K.C., Sweetman, A.J., 2008. A first global production, emission, and
472 environmental inventory for perfluorooctane sulfonate. *Environmental Science & Technology* 43,
473 386-392.

474 Peng, C., Zhou, X., Zhao, S., Wang, X., Zhu, B., Piao, S., Fang, J., 2009. Quantifying the response
475 of forest carbon balance to future climate change in Northeastern China: model validation and
476 prediction. *Global and Planetary Change* 66, 179-194.

477 Prevedouros, K., Jones, K., Sweetman, A., 2004a. European-scale modeling of concentrations and
478 distribution of polybrominated diphenyl ethers in the pentabromodiphenyl ether product.
479 *Environmental science & technology* 38, 5993-6001.

480 Prevedouros, K., MacLeod, M., Jones, K.C., Sweetman, A.J., 2004b. Modelling the fate of
481 persistent organic pollutants in Europe: parameterisation of a gridded distribution model.
482 *Environmental Pollution* 128, 251-261.

483 Song, S., Su, C., Lu, Y., Wang, T., Zhang, Y., Liu, S., 2016. Urban and rural transport of
484 semivolatile organic compounds at regional scale: A multimedia model approach. *Journal of*
485 *Environmental Sciences* 39, 228-241.

486 Tao, Y., Li, F., Wang, R., Zhao, D., 2015. Effects of land use and cover change on terrestrial
487 carbon stocks in urbanized areas: a study from Changzhou, China. *Journal of Cleaner Production*
488 103, 651-657.

489 Teran, T., Lamon, L., Marcomini, A., 2012. Climate change effects on POPs' environmental
490 behaviour: a scientific perspective for future regulatory actions. *Atmospheric Pollution Research* 3,
491 466-476.

492 Wang, P., Lu, Y., Wang, T., Fu, Y., Zhu, Z., Liu, S., Xie, S., Xiao, Y., Giesy, J.P., 2014.
493 Occurrence and transport of 17 perfluoroalkyl acids in 12 coastal rivers in south Bohai coastal
494 region of China with concentrated fluoropolymer facilities. *Environmental pollution* 190, 115-122.

495 Wang, P., Lu, Y., Wang, T., Zhu, Z., Li, Q., Zhang, Y., Fu, Y., Xiao, Y., Giesy, J.P., 2015.
496 Transport of short-chain perfluoroalkyl acids from concentrated fluoropolymer facilities to the
497 Daling River estuary, China. *Environmental Science and Pollution Research* 22, 9626-9636.

498 Wang, W., Simonich, S.L.M., Xue, M., Zhao, J., Zhang, N., Wang, R., Cao, J., Tao, S., 2010.
499 Concentrations, sources and spatial distribution of polycyclic aromatic hydrocarbons in soils from
500 Beijing, Tianjin and surrounding areas, North China. *Environmental Pollution* 158, 1245-1251.

501 Woehrschimmel, H., MacLeod, M., Hungerbuhler, K., 2013. Emissions, Fate and Transport of
502 Persistent Organic Pollutants to the Arctic in a Changing Global Climate. *Environmental Science*
503 & Technology 47, 2323-2330.

504 Woodfine, D.G., MacLeod, M., Mackay, D., Brimacombe, J.R., 2001. Development of continental
505 scale multimedia contaminant fate models: integrating GIS. *Environmental Science and Pollution*
506 *Research* 8, 164-172.

507 Xie, S., Lu, Y., Wang, T., Liu, S., Jones, K., Sweetman, A., 2013a. Estimation of PFOS emission
508 from domestic sources in the eastern coastal region of China. *Environment international* 59,
509 336-343.

510 Xie, S., Wang, T., Liu, S., Jones, K.C., Sweetman, A.J., Lu, Y., 2013b. Industrial source
511 identification and emission estimation of perfluorooctane sulfonate in China. *Environment*
512 *international* 52, 1-8.

513 Yang, L., Zhu, L., Liu, Z., 2011. Occurrence and partition of perfluorinated compounds in water
514 and sediment from Liao River and Taihu Lake, China. *Chemosphere* 83, 806-814.

515 Zhang, L., Wu, T., Xin, X., Dong, M., Wang, Z., 2012. Projections of annual mean air temperature

516 and precipitation over the globe and in China during the 21st century by the BCC Climate System
517 Model BCC_CSM1.0. *Acta Meteorologica Sinica* 26, 362-375.

518 Zhao, X., Xia, X., Zhang, S., Wu, Q., Wang, X., 2014. Spatial and vertical variations of
519 perfluoroalkyl substances in sediments of the Haihe River, China. *Journal of Environmental*
520 *Sciences* 26, 1557-1566.

521 Zhao, Z., Tang, J., Xie, Z., Chen, Y., Pan, X., Zhong, G., Sturm, R., Zhang, G., Ebinghaus, R.,
522 2013. Perfluoroalkyl acids (PFAAs) in riverine and coastal sediments of Laizhou Bay, North
523 China. *Science of the total environment* 447, 415-423.

524 Zhou, Z., Ma, L., 2013. Research advance of climate change influence on environmental behavior
525 of POPs. *Environmental Pollution & Control* 35, 84-87.

526 Zhu, Z., Wang, T., Wang, P., Lu, Y., Giesy, J.P., 2014. Perfluoroalkyl and polyfluoroalkyl
527 substances in sediments from South Bohai coastal watersheds, China. *Marine pollution bulletin* 85,
528 619-627.

529